HHS Public Access

Author manuscript

Genesis. Author manuscript; available in PMC 2017 February 06.

Published in final edited form as:

Genesis. 2015 September ; 53(9): 604–611. doi:10.1002/dvg.22880.

Rfx2 is required for spermatogenesis in the mouse

William Shawlot[1], **Mercedes Vazquez-Chantada**[1], **John B. Wallingford**[2,3], and **Richard H. Finnell**[1]

[1]Department of Nutritional Sciences, The Dell Pediatric Research Institute, The University of Texas at Austin

[2]Department of Molecular Biosciences, The University of Texas at Austin

[3]Howard Hughes Medical Institute, The University of Texas at Austin

Abstract

RFX transcription factors are key regulators of ciliogenesis in vertebrates. In *Xenopus* and zebrafish embryos, knockdown of *Rfx2* causes defects in neural tube closure and in left-right axis patterning. To determine the essential role of the *Rfx2* gene in mammalian development, we generated *Rfx2*-deficient mice using an embryonic stem cell clone containing a *lacZ* gene trap reporter inserted into the first intron of the *Rfx2* gene. We found that the *Rfx2 lacZ* reporter is expressed in ciliated tissues during mouse development including the node, the floor plate and the dorsal neural tube. However, mice homozygous for the *Rfx2* gene trap mutation did not have defects in neural tube closure or in organ *situs*. The gene trap insertion appears to create a null allele as *Rfx2* mRNA was not detected in $Rfx2^{gt/gt}$ embryos. Although *Rfx2*-deficient mice do not have an obvious embryonic phenotype, we found that $Rfx2^{gt/gt}$ males are infertile due to a defect in spermatid maturation at or before the round and elongating spermatid stage. Our results indicate that *Rfx2* is not essential for embryonic development in the mouse but is required for spermatogenesis.

Keywords

gene trap; ciliogenesis; node; neural tube; male fertility

RESULTS AND DISCUSSION

Cilia are microtubule-based organelles that project from the surface of cells and play an important role in cellular signaling (Berbari *et al.*, 2009). During development, cilia located in the node and in the floor plate are important in left-right axis formation and in dorsal-ventral patterning of the neural tube, respectively (Eggenschwiler and Anderson, 2007; Hirokawa *et al.*, 2006). Recent work indicates that the *Rfx2* transcription factor regulates the expression of a ciliogenic gene program necessary for proper neural tube closure in *Xenopus,* and for left-right axis specification in both zebrafish and *Xenopus* embryos (Bisgrove *et al.*, 2012; Chung *et al.*, 2012). To determine the essential role of the mammalian

Corresponding Author: William Shawlot, 1 512 471-3918 (phone), wshawlot@austin.utexas.edu, Institute for Cellular and Molecular Biology, 1 University Station, A4800, Austin, TX 78712.

Rfx2 gene we generated an *Rfx2* gene trap mouse line using a C57BL/6N gene-trap clone, IST10638H11, obtained from the Texas A&M Institute for Genomic Medicine. The ES cell clone contains a *lacZ* reporter poly A gene cassette with a splice acceptor inserted into intron 1 of the *Rfx2* gene before the ATG start codon in exon 2 (Fig. 1). Transcription at the locus should result in the splicing of exon 1 to the gene trap vector and eliminate the production of the endogenous transcript. This mutation is predicted to create a null allele and the expression of the *lacZ* gene should mimic the expression of the *Rfx2* gene.

To determine the expression pattern of *Rfx2*, we performed X-gal staining on embryos from timed matings between $Rfx2^{gt/+}$ males and CD-1 females. At embryonic day (E) 7.0, *lacZ* activity was detected in the anterior primitive streak preceding the morphological appearance of the node, and at E7.5 in the node and in the midline notochordal plate cells extending anteriorly from the node (Fig. 2a,b). At E8.5, *lacZ* activity was present in the node now located in the tail region (Fig. 2c), consistent with previous results using RNA *in situ* hybridization to *Rfx2* (Bisgrove *et al.*, 2012). That previous study of *Rfx2* expression in the mouse focused largely on expression in the node. Notably, using our *lacZ* allele, we also observed that at E9.5, X-gal staining was detected in the floor plate and in the dorsal portion of the neural tube, with the area of highest expression in the anterior portion of the spinal cord. Staining was also detected in the developing gut (Fig. 2d–f). At E10.5, an additional staining region was observed in the telencephalon region of the brain and at E12.5 *lacZ* activity was also observed in the anterior portion of the limb bud (Fig. 2g,h).

To determine whether $Rfx2^{gt/gt}$ mice were viable we performed heterozygous intercrosses on both C57BL/6N and C57BL/6N x CD-1 genetic backgrounds and genotyped the resulting mice at weaning. We obtained wild-type, heterozygous and homozygous *Rfx2* mice at approximately the expected ratio of 1:2:1 (Table 1). We also observed that the stomach, as indicated by the milk spot, was correctly located on the left side in all pups examined (76 pups, 11 litters) from heterozygous by heterozygous crosses. This suggests that the *Rfx2* mutation does not cause *situs inversus*. We also examined embryos from matings between mice heterozygous for the gene trap allele at E10.5 and found no obvious morphological differences between $Rfx2^{+/+}$ and $Rfx2^{gt/gt}$ littermate embryos (data not shown). Adult $Rfx2^{gt/gt}$ mice appeared morphologically normal and did not display any obvious abnormal behaviors. These results indicate that mice homozygous for the *Rfx2* gene trap allele are viable and do not have any obvious structural malformations.

One possible explanation for the lack of an embryonic phenotype is that the gene-trap mutation does not create a null allele. To determine whether *Rfx2* mRNA is present in $Rfx2^{gt/gt}$ embryos we performed reverse transcription polymerase chain reaction (RT-PCR) using total RNA from E9.5 stage embryos. We used primers that amplify cDNA sequences downstream of the gene trap that correspond to exons 8 through 12, which encompasses part of the DNA binding domain of Rfx2. A band of the predicted size of 494 bp was observed in the $Rfx2^{+/+}$ cDNA sample but no band was observed in the $Rfx2^{gt/gt}$ cDNA sample. (Fig. 3). Hypoxanthine guanine phosphoribosyl transferase (HPRT) was used as a control for the quality of the cDNA samples and amplification was observed in both $Rfx2^{+/+}$ and $Rfx2^{gt/gt}$ samples. The absence of detectable *Rfx2* mRNA suggests that the gene trap insertion creates a null allele and that *Rfx2* is not essential for embryonic development in the mouse. We also

note that embryonic development appears to be normal in an independently generated *Rfx2* knockout mouse line (Kistler *et al.*, 2015).

To determine whether mice homozygous for the gene trap were fertile, we crossed four $Rfx2^{gt/gt}$ females with littermate $Rfx2^{+/+}$ males and eight $Rfx2^{gt/gt}$ males with $Rfx2^{+/+}$ littermate females. All four $Rfx2^{gt/gt}$ females were fertile, however none of the eight $Rfx2^{gt/gt}$ males were fertile although all displayed normal mating and plugging behavior. $Rfx2^{gt/gt}$ males on both C57BL/6N and C57BL/6N x CD-1 genetic backgrounds were analyzed. We next attempted to recover sperm from the caudal epididymis of 12 week old $Rfx2^{gt/+}$ and $Rfx2^{gt/gt}$ males. Although abundant sperm was recovered from littermate $Rfx2^{gt/+}$ males, $Rfx2^{gt/gt}$ males completely lacked sperm. To determine whether the lack of sperm in the epididymis was due to a defect in sperm production or sperm transport to the epididymis, we examined histological sections of testes from $Rfx2^{gt/+}$ and $Rfx2^{gt/gt}$ mice. We observed abundant spermatozoa in the seminiferous tubules of $Rfx2^{gt/+}$ mice but no spermatazoa was present in the seminiferous tubules of $Rfx2^{gt/gt}$ mice. Instead, we observed an accumulation of abnormal symplasts of round spermatids (Fig. 4a–d). Spermatogonial cells and spermatocytes were present in the $Rfx2^{gt/gt}$ testis and were not obviously abnormal. We did note that in the $Rfx2^{gt/gt}$ testis sections there appeared to be an increase in the number of Leydig cells in the interstitial space (Fig. 4e,f).

To confirm that early spermatid development was affected, we analyzed the expression of several marker genes expressed in spermatocytes and spermatids by quantitative PCR (qPCR). The transcription factor genes *A-myb* (*Mybl1*) and *Crem* encode transcription factors expressed in spermatocytes (Foulkes *et al.*, 1992; Mettus *et al.*, 1994). Both *A-myb* and *Crem* (*Crem-tau* isoform) were expressed in the testis of $Rfx2^{gt/gt}$ mice at levels roughly equivalent to levels in the testis from $Rfx2^{+/+}$ mice (Fig. 5 a,b). We next examined the expression of *Tnp1* and *Tnp2*, which encode proteins involved in chromatin condensation and whose mRNAs are present in round and elongating spermatids (Kleene, 1989). We found that *Tnp1* and *Tnp2* expression levels were dramatically reduced in $Rfx2^{gt/gt}$ mice compared to $Rfx2^{+/+}$ mice (Fig. 5 c,d). These results suggest that the differentiation of spermatids is abnormal before or at the round and elongating spermatid stage. We also examined the expression of two putative Rfx2 target genes, the variant general transcription factor gene *Alf* (*GTF2a1l*) and the histone *H1t* gene (*Hist1h1t*) (Horvath *et al.*, 2004; Horvath *et al.*, 2009; Wolfe *et al.*, 2004). We found that although the average expression levels of both genes was lower in the KO samples, the standard deviations for both wild-type and KO samples overlapped (Fig. 5e,f).

Our findings indicate that *Rfx2* is not essential for embryonic development in the mouse but is required for male fertility. The lack of a left-right patterning defect or neural tube closure defect may be due to functional redundancy with other Rfx family members. There are seven Rfx family members and they contain a highly conserved DNA binding domain (Aftab *et al.*, 2008; Emery *et al.*, 1996, Reith *et al.*, 1994; Steimle *et al.*, 1995). *Rfx3* has previously been shown to be expressed in the node (Bonnafe et al., 2004). Consistent with the possibility of overlapping function between *Rfx2* and *Rfx3*, loss of *Rfx3* does not eliminate nodal cilia but rather results in shortening of the cilia and a partially penetrant *situs inversus* phenotype (Bonnafe *et al.*, 2004). In the neural tube, *Rfx4* may substitute for the absence of *Rfx2* as

Rfx4 is uniformly expressed throughout the neuroepithelium before neural tube closure. In mice with a point mutation in the dimerization domain of *Rfx4*, cilia still form but they are stunted and embryos display patterning defects in the ventral spinal cord (Ashique *et al.*, 2009).

The defect in spermatogenesis we observed is consistent with the published data on *Rfx2* expression in the testis (Horvath *et al.*, 2004; Kistler *et al.*, 2009; Wolfe *et al.*, 2004). Rfx2 protein is present in pachytene spermatocytes and round spermatids, but it is not present in Sertoli cells or in human Leydig cells (Horvath *et al.*, 2004, http://www.proteinatlas.org/ENSG00000087903-RFX2/tissue/testis#img). This suggests that the defect is intrinsic to pachytene spermatocytes and early spermatids. Although Rfx factors control the expression of many genes essential for the assembly of ciliary and flagellar axonemes (Ashique *et al.*, 2009; Chung *et al.*, 2012; El Zein *et al.*, 2009), testis histology is largely normal and elongated spermatids lacking flagella can be observed in male-sterile mice with targeted mutations in axoneme components (Yan, 2009). This suggests that *Rfx2* regulates additional cilia-independent gene programs during spermatid development. Indeed, Rfx2 controls cell movement and cell remodeling gene programs in addition to ciliogenesis during the maturation of *Xenopus* multi-ciliated cells (MCCs) (Chung *et al*; 2014). The testis phenotype in *Rfx2* mice resembles the symplastic spermatid phenotype of *Fndc3a*-deficient mice (MacGregor *et a*l., 1990; Obholz *et al.*, 2006). Although there do not appear to be Rfx2 binding sites in the promoter region of the mouse *Fndc3a* gene (G. MacGregor, personal communication), the related gene, *Fndc3b*, is a direct target of Rfx2 in MCCs. It is possible therefore, that the genetic program for the maturation of nascent spermatids shares elements with the development of MCCs and that both programs are under *Rfx2* control.

METHODS

Generation of *Rfx2* gene trap mice

Chimeric mice were made by the aggregating clumps of approximately 6–12 ES cells with 8-cell stage CD-1 embryos (Gertsenstein *et al.*, 2010). ES cells were grown in RESGRO culture medium (EMD Millipore) for 2 passages before aggregation. Embryos were transferred to recipient females and high percentage male chimeras were mated to C57BL/6N females to obtain mice heterozygous for the gene trap allele. Pups were genotyped by PCR. The primers used were: Rfx2 Fw1 = GGTCTGGAACCAACCCTT CT, Rfx2 Rv1 = CAGGATTCCTTGGCAACAGT, and LTRrev2 = CCAATAAACCCTCTT GCAGTTGC. The wild-type allele generates a 267 bp band and the gene trap allele generates a 139 bp band. The PCR cycling parameters were 95° C for 30 seconds, then 35 cycles at 95° C for 10 seconds, 60° C for 30 seconds, 65° C for 1 minute and a final extension at 65° C for 5 minutes using LongAmp DNA polymerase (New England Biolabs). Mice were maintained on both C57BL/6N and C57BL/6N x CD1 genetic backgrounds. All animal procedures were approved by The University of Texas at Austin Institutional Animal Care and Use Committee. *Rfx2*^{gt}/+ sperm on a C57BL/6N background is available from the Texas A&M Institute for Genomic Medicine knockout mouse repository.

Staining for β-galactosidase (*lacZ*) activity

Embryos were fixed in 0.2% glutaraldehyde-based fix and stained according to the protocol in *Manipulating the Mouse Embryo* 2nd edition (Hogan *et al.*, 1994).

Testis histology

Testes were fixed in 4% paraformaldehyde overnight. Paraffin embedding, sectioning and staining was done by the Histology core at The University of Texas at Austin Dell Pediatric Research Institute as a fee for service.

RT-PCR and qPCR

For RT-PCR, total RNA was isolated from E9.5 embryos using Trizol reagent (Life Technologies). The genotype of each embryo was determined by PCR analysis using DNA isolated from the yolk sac. RNA was reverse transcribed using random primers and M-MuLV reverse transcriptase (New England Biolabs). The primers used for PCR were: exon 8F = GAACCGACTGCAGGAAGACA and exon 12R = TCCACTGTAGGATCGGCTCA. The HPRT primers were CACAGGACTAGAACACCTGC and GCTGGTGAAAAGGACCTCT (Keller et al., 1993). The PCR cycling parameters were as described above for genotyping.

For qPCR, total RNA was extracted from 3 *Rfx2*$^{+/+}$ and 3 *Rfx2*$^{gt/gt}$ mice on a C57BL/6N background at 2–3 months of age with the Allprep DNA/RNA Mini Kit (Qiagen). The RNA was treated with DNaseI (Invitrogen) and then reverse transcribed using Superscript III (Invitrogen) according to the manufacture's instructions. A portion of the synthesized cDNA was diluted to generate a standard curve for qPCR reaction. qPCRs were performed using an Applied Biosystems thermocycler. Cycle threshold values were analyzed and normalized to the housekeeping transcripts *9S* ribosomal phosphoprotein and *GAPDH* (Ginzinger, 2002; Huggett *et al.*, 2005). The *GAPDH* primers sequences were: GAPDH L: GAGTCAACGGATTTGGTCGT and GAPDH R: TTGATTTTGGAGGGATCTCG. The *9S* primer sequences were: 9s L: GACTCCGGAACAAACGTGAGGT and 9s R: CTTCATCTTGCCCTCGTCCA. The sequence of the primers for testis marker genes were: A-myb F = CGTTGGGCCGAGATTGCTAA and A-myb R = CACAATTGCCATCAGGCGAC, Tnp1F = CATGGCATGAGGAGAGGCAA and Tnp1R = GCCCCGTGTTGTTTGAAGAC, Tnp2F = TCGACACTCACCTGCAAGAC and Tnp2R = ATCCTGGAGTGCGTCACTTG. The Crem primers (Cat. No./ID QT01055782), Gtf2a1l (Cat./ID: QT00121604,) and Hist1h1t (Cat No./ID: QT00250201) were purchased from Qiagen. The Crem primers recognize *Crem tau* isoforms (NM_001110856.2, NM_001271504.1, NM_001271505.1, NM_001271506.1). Quantitative PCR reactions and standard curve dilutions were analyzed in triplicate. The cycling conditions were: 94° C for 15 seconds, 60° C for 30 seconds performed for 40 cycles. The specificity of the PCR products was determined by their melting curves. Ct values were extrapolated to a standard curve performed simultaneously with the samples and the data were normalized to the expression of the housekeeping genes *GAPDH* and *9S*. Since the Ct values obtained for both housekeeping genes were very similar, a median value of the 2 housekeeping Ct values was used to normalize the expression levels of the target genes.

Acknowledgments

We thank Rebecca Fitch in the Histology core at The University of Texas at Austin Dell Pediatric Research Institute for sectioning and staining testis samples. We thank Grant MacGregor for his thoughts on the *Rfx2* testis phenotype, information on the *Fndc3a* mouse mutant, and comments on the manuscript. This work was funded in part with grant support from the National Institutes of Health (P01HD067244, R01NS076465) to RHF. JBW is supported by the NHLBI (R01HL117164) and is an Early Career Scientist of the HHMI.

National Institutes of Health (P01HD067244, R01NS076465) to RHF

National Institutes of Health (R01HL117164) and Howard Hughes Medical Institute to JBW

LITERATURE CITED

Aftab S, Semenec L, Chu JS, Chen N. Identification and characterization of novel human tissue-specific RFX transcription factors. BMC Evol Biol. 2008; 8:226. [PubMed: 18673564]

Ashique AM, Choe Y, Karlen M, May SR, Phamluong K, Solloway MJ, Ericson J, Peterson AS. The Rfx4 transcription factor modulates Shh signaling by regional control of ciliogenesis. Sci Signal. 2009; 2:ra70. [PubMed: 19887680]

Berbari NF, O'Connor AK, Haycraft CJ, Yoder BK. The primary cilium as a complex signaling center. Curr Biol. 2009; 19:R526–R535. [PubMed: 19602418]

Bisgrove W, Makova S, Yost JH, Brueckner M. RFX2 is essential in the ciliated organ of asymmetry and an RFX2 transgene identifies a population of ciliated cells sufficient for fluid flow. Dev Biol. 2012; 363:166–178. [PubMed: 22233545]

Bonnafe E, Touka M, AitLounis A, Baas D, Barras E, Ucla C, Moreau A, Flamant F, Dubruille R, Couble P, Collignon J, Durand B, Reith W. The transcription factor RFX3 directs nodal cilium development and left-right asymmetry specification. Mol Cell Biol. 2004; 24:4417–4427. [PubMed: 15121860]

Chung MI, Peyrot SM, LeBoeuf S, Park TJ, McGary KL, Marcotte EM, Wallingford JB. RFX2 is broadly required for ciliogenesis during vertebrate development. Dev Biol. 2012; 363:155–165. [PubMed: 22227339]

Chung MI, Kwon T, Tu F, Brooks ER, Gupta R, Meyer M, Marcotte EM, Wallingford JB. Coordinated genomic control of ciliogenesis and cell movement by Rfx2. eLIFE. 2014:32014.

Eggenschwiler JT, Anderson KV. Cilia and developmental signaling. Annu Rev Cell Dev Biol. 2007; 23:345–373. [PubMed: 17506691]

El Zein L, Ait-Lounis A, Morle L, Thomas J, Chhin B, Spassky N, Reith W, Durand B. RFX3 governs growth and beating efficiency of motile cilia in mouse and controls the expression of genes involved in human ciliopathies. J Cell Sci. 2009; 122:3180–3189. [PubMed: 19671664]

Emery P, Durand B, Mach B, Reith W. RFX proteins, a novel family of DNA binding proteins conserved in the eukaryotic kingdom. Nucleic Acids Res. 1996; 24:803–807. [PubMed: 8600444]

Foulkes NS, Mellstrom B, Benusiglio E, Sassone-Corsi P. Developmental switch of CREM function during spermatogenesis: from antagonist to activator. Nature. 1992; 355:80–84. [PubMed: 1370576]

Gertsenstein M, Nutter LM, Reid T, Pereira M, Stanford WL, Rossant J, Nagy A. Efficient generation of germ line transmitting chimeras from C57BL/6N ES cells by aggregation with outbred host embryos. PLoS One. 2010; 5:e11260. [PubMed: 20582321]

Ginzinger DG. Gene quantification using real-time quantitative PCR: an emerging technology hits the mainstream. Exp Hematol. 2002; 30:503–512. [PubMed: 12063017]

Hirokawa N, Tanaka Y, Okada Y, Takeda S. Nodal flow and the generation of left-right asymmetry. Cell. 2006; 125:33–45. [PubMed: 16615888]

Hogan, B., Beddington, R., Costantini, F., Lacy, E. Manipulating the Mouse Embryo: A Laboratory Manual. Cold Spring Harbor Laboratory Press; 1994. p. 373-375.

Horvath GC, Kistler WS, Kistler MK. RFX2 is a potential transcriptional regulatory factor for histone H1t and other genes expressed during the meiotic phase of spermatogenesis. Biol Reprod. 2004; 71:1551–1559. [PubMed: 15229132]

Horvath GC, Kistler MK, Kistler WS. RFX2 is a candidate downstream amplifier of A-MYB regulation in mouse spermatogenesis. BMC Dev Biol. 2009; 9:63. [PubMed: 20003220]

Huggett J, Dheda K, Bustin S, Zumla A. Real-time RT-PCR normalisation; strategies and considerations. Genes Immun. 2005; 6:279–284. [PubMed: 15815687]

Keller G, Kennedy M, Papayannopoulou T, Wiles MV. Hematopoietic commitment during embryonic stem cell differentiation in culture. Mol Cell Biol. 1993; 13:473–486. [PubMed: 8417345]

Kleene KC. Poly(A) shortening accompanies the activation of translation of five mRNAs during spermiogenesis in the mouse. Development. 1989; 106:367–373. [PubMed: 2512111]

Kistler WS, Horvath GC, Dasgupta A, Kistler MK. Differential expression of Rfx1-4 during mouse spermatogenesis. Gene Expr Patterns. 2009; 9:515–519. [PubMed: 19596083]

Kistler WS, Baas D, Lemeille S, Paschaki M, Seguin-Estevez Q, Barras E, Ma W, Duteyrat J-L, Morie L, Durand B, Reith W. RFX2 is a major transcriptional regulator of spermiogenesis. PLOS Genetics. 2015 doi:10.1371.

MacGregor GR, Russell LD, Van Beek ME, Hanten GR, Kovac MJ, Kozak CA, Meistrich ML, Overbeek PA. Symplastic spermatids (sys): a recessive insertional mutation in mice causing a defect in spermatogenesis. Proc Natl Acad Sci U S A. 1990; 87:5016–5020. [PubMed: 2164218]

Mettus RV, Litvin J, Wali A, Toscani A, Latham K, Hatton K, Reddy EP. Murine A-myb: evidence for differential splicing and tissue-specific expression. Oncogene. 1994; 9:3077–3086. [PubMed: 8084617]

Obholz KL, Akopyan A, Waymire KG, MacGregor GR. FNDC3A is required for adhesion between spermatids and Sertoli cells. Dev Biol. 2006; 298:498–513. [PubMed: 16904100]

Reith W, Ucla C, Barras E, Gaud A, Durand B, Herrero-Sanchez C, Kobr M, Mach B. RFX1, a transactivator of hepatitis B virus enhancer I, belongs to a novel family of homodimeric and heterodimeric DNA-binding proteins. Mol Cell Biol. 1994; 14:1230–1244. [PubMed: 8289803]

Steimle V, Durand B, Barras E, Zufferey M, Hadam MR, Mach B, Reith W. A novel DNA-binding regulatory factor is mutated in primary MHC class II deficiency (bare lymphocyte syndrome). Genes Dev. 1995; 9:1021–1032. [PubMed: 7744245]

Wolfe SA, Wilkerson DC, Prado S, Grimes SR. Regulatory factor X2 (RFX2) binds to the H1t/TE1 promoter element and activates transcription of the testis-specific histone H1t gene. J Cell Biochem. 2004; 91:375–383. [PubMed: 14743396]

Yan W. Male infertility caused by spermiogenic defects: lessons from gene knockouts. Mol Cell Endocrinol. 2009; 306:24–32. [PubMed: 19481682]

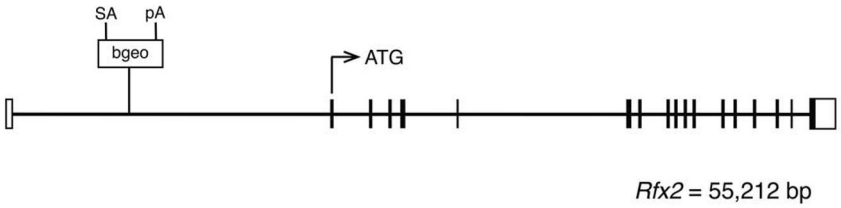

FIG 1.

Rfx2 gene trap allele. The gene trap vector containing a βgeo cassette with a splice acceptor (SA) and poly A (pA) sequence is inserted into intron 1 before the ATG start codon in exon 2. The βgeo gene trap cassette is not drawn to scale.

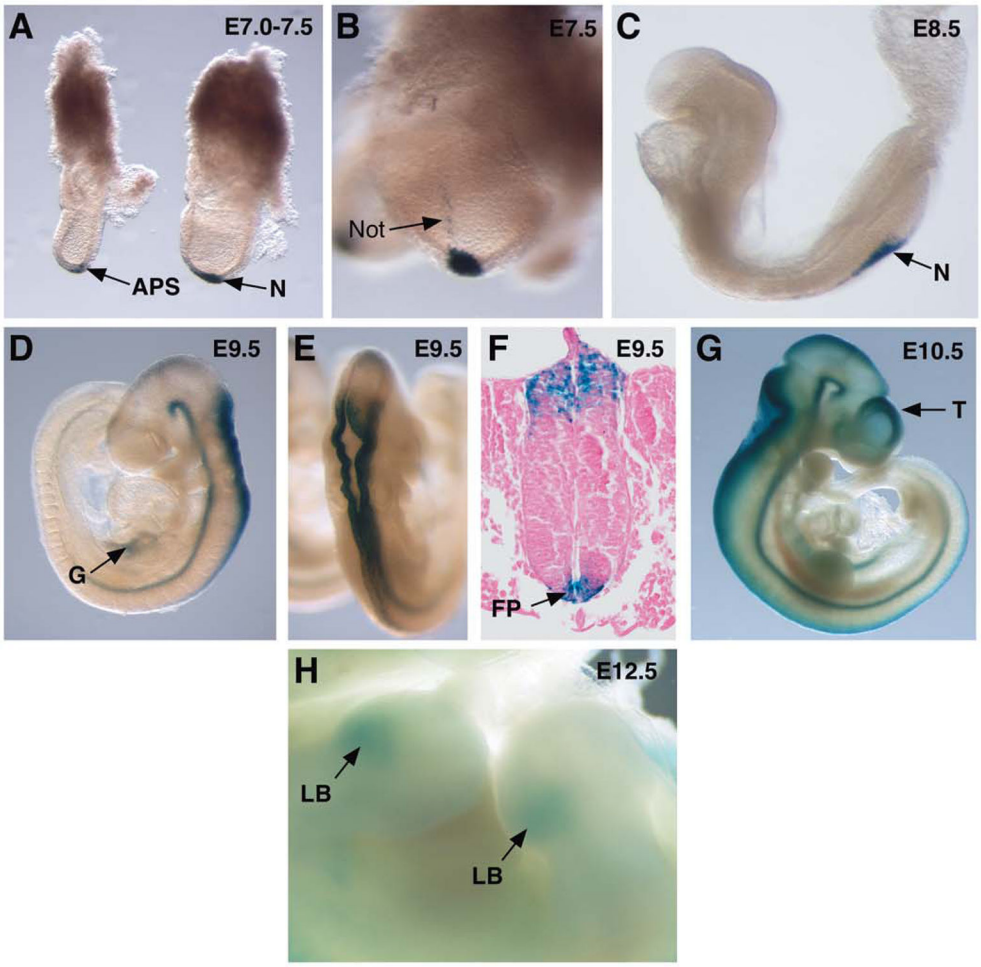

FIG 2.

Expression of *Rfx2* between E7.0 and E12.5 as revealed by X-gal staining for *lacZ* activity. **(a)** At E7.0 – 7.5 *lacZ* activity is present in the anterior primitive streak region prior to the morphological appearance of the node (E7.0) and then in the definitive node (E7.5). **(b)** E7.5 embryo showing *lacZ* activity in the node and the midline notochordal plate extending anteriorly from the node. **(c)** E8.5 embryo with *lacZ* activity in the node localized to the tail region. **(d–f)** E9.5 embryo showing *lacZ* activity in the dorsal neural tube and the floor plate and in the gut region. **(g)** E10.5 embryo with a new expression domain in the telencephalon. **(h)** E12.5 embryo with expression in the anterior portion of the fore and hind limb buds. APS = anterior primitive streak, N = node, Not = notochordal plate, G = gut, FP = floor plate, T = telencephalon, LB = limb bud.

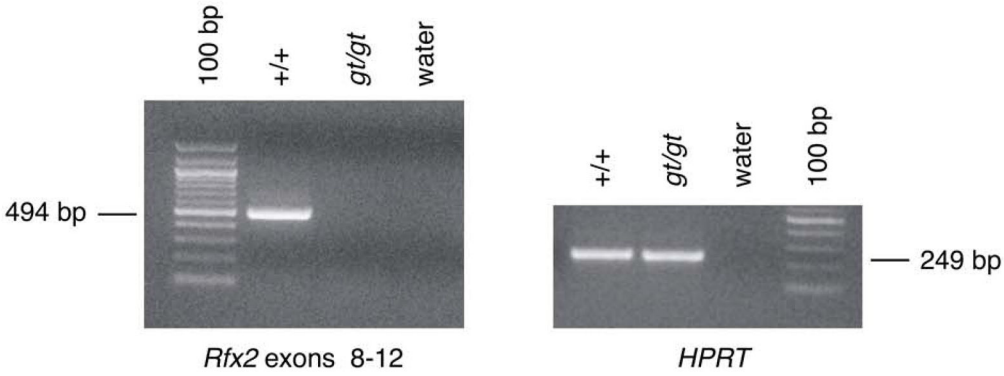

FIG 3.

RT-PCR analysis of *Rfx2* expression in E9.5 $Rfx2^{+/+}$ and $Rfx2^{gt/gt}$ embryos. PCR was performed with primers than amplify sequences spanning exons 8 through 12. The amplified *Rfx2* cDNA band is 494 base pairs (bp). In the mouse genome the primer sequences are separated by 2993 bp of genomic DNA. *HPRT* was used as a positive control for the quality of the synthesized first strand cDNA and amplify a band of 249 bp. The HPRT primers amplify a band of ~1100 bp in genomic DNA (not shown).

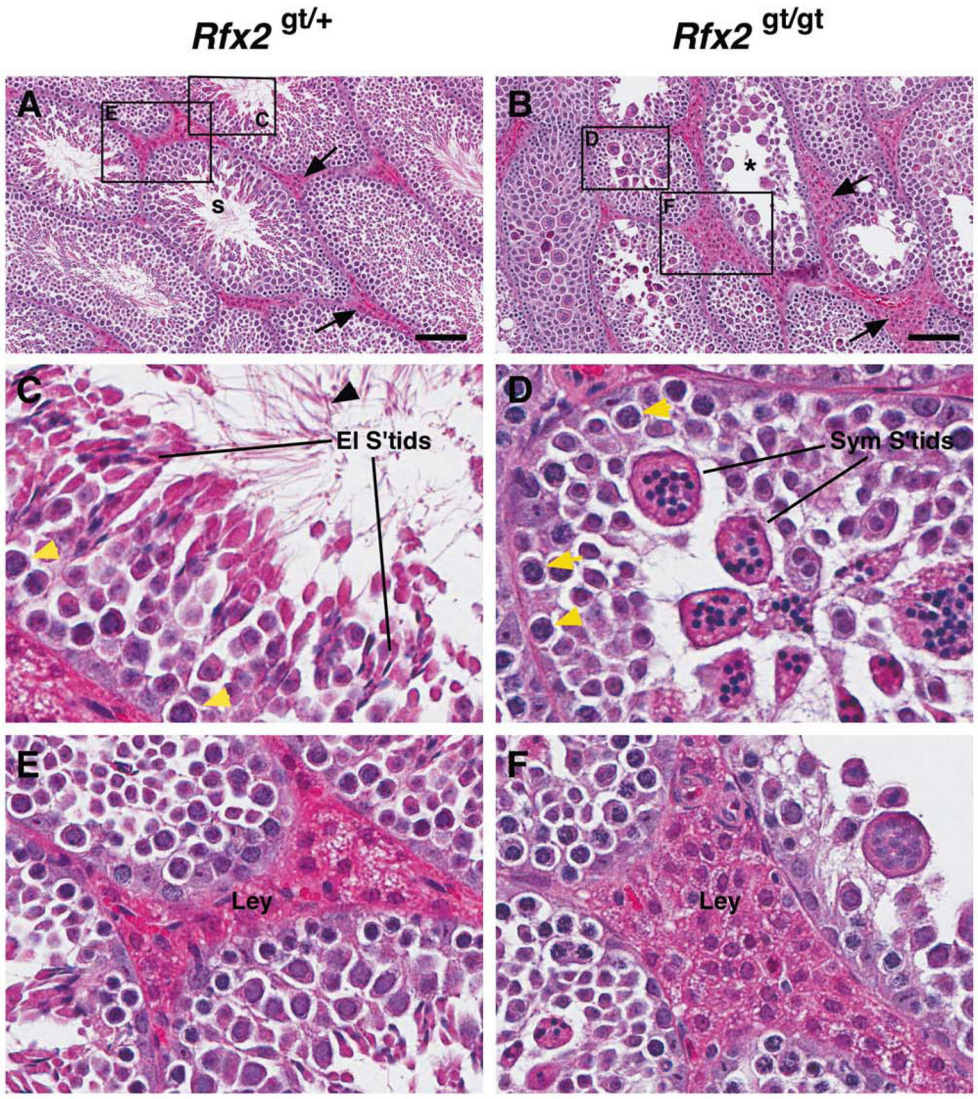

FIG 4.

Rfx2$^{gt/+}$ and *Rfx2*$^{gt/gt}$ testis histology. Panels A, C and E correspond to *Rfx2*$^{gt/+}$. Panels B, D, and F correspond to *Rfx2*$^{gt/gt}$. The boxed areas in panels A and B are enlarged in panels C–F. **(a,b)** Spermatozoa (s) are present in the lumen of seminiferous tubules from *Rfx2*$^{gt/+}$ mice but are absent in *Rfx2*$^{gt/gt}$ testis (*****). The arrows point to the interstitial space containing Leydig cells, which appear enlarged in *Rfx2*$^{gt/gt}$ mice compared to *Rfx2*$^{gt/+}$ mice. The bar equals 100 μm. **(c,d)** Elongating spermatids (El S'tids) are prominent in the seminiferous tubules of *Rfx2*$^{gt/+}$ testis and give rise to spermatozoa (arrowhead). In *Rfx2*$^{gt/gt}$ testis, elongating spermatids are replaced by symplasts of spermatids (Sym S'tids). Spermatocytes located basally (yellow arrowheads) are present in both *Rfx2*$^{gt/+}$ and *Rfx2*$^{gt/gt}$ testis sections. **(e,f)** Increased numbers of Leydig cells (Ley) are present in the interstitial space of *Rfx2*$^{gt/gt}$ testis compared with *Rfx2*$^{gt/+}$ testis.

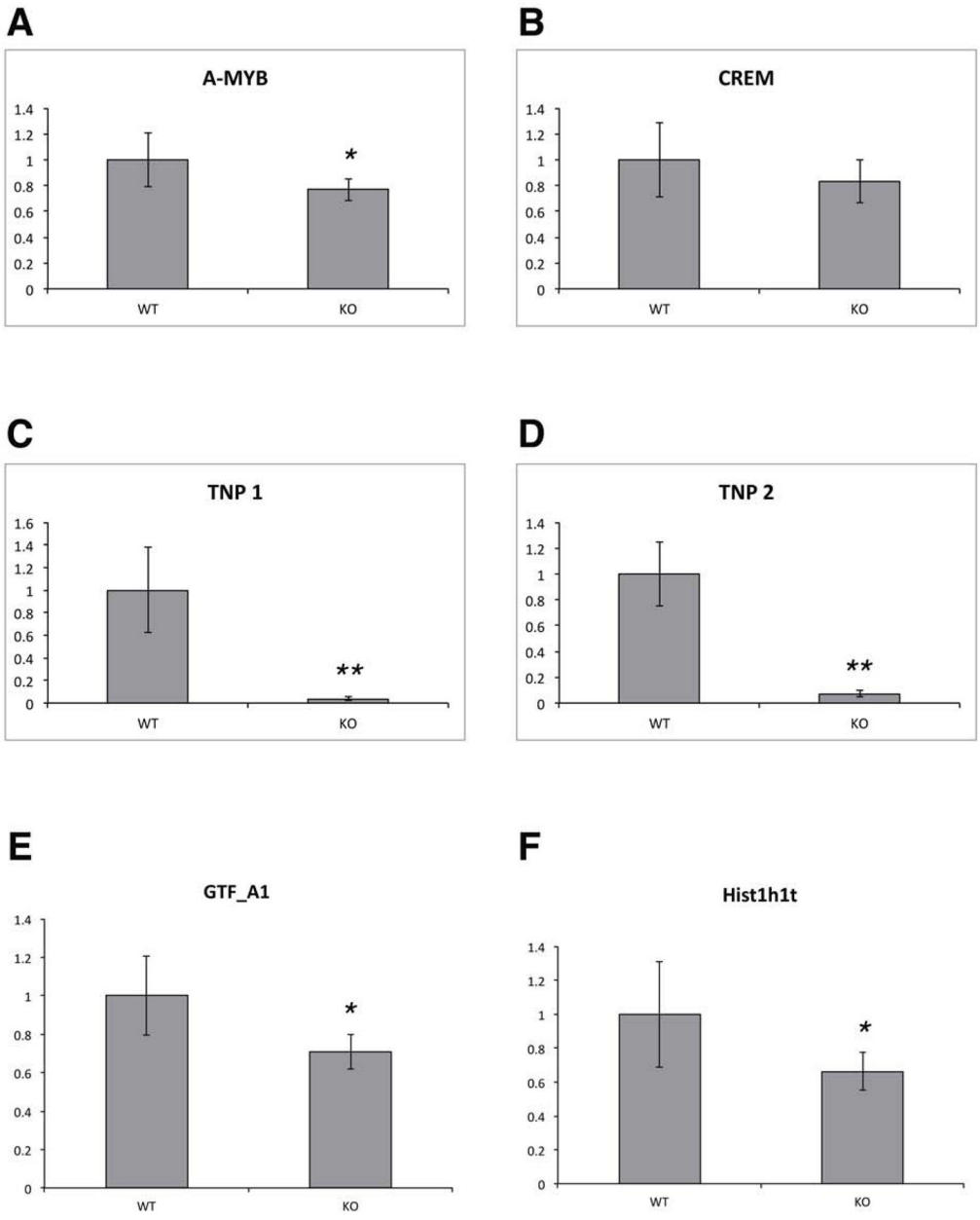

FIG 5.

Analysis of sperm marker gene expression in *Rfx2*$^{+/+}$ and *Rfx2*$^{gt/gt}$ mice by qPCR. **(a,b)** No significant difference in the expression levels of *A-myb* and *Crem* was observed in *Rfx2*$^{gt/gt}$ mice compared to *Rfx2*$^{+/+}$ mice. **(c,d)** Expression of marker genes *Tnp1* and *Tnp2* were down-regulated in the testis of *Rfx2*$^{gt/gt}$ mice compared with *Rfx2*$^{+/+}$ mice. **(e,f)** The average expression values of *GTF_A1*(*Gtf2a1l*) and *Hist1h1t* were lower in KO samples than in wild-type samples but the standard deviations overlapped. mRNA expression was normalized to *Gapdh* and *9s* mRNA for qPCR analysis. **P* <0.05, ***P*<0.005.

Table 1

Genotype of mice at weaning from *Rfx2*$^{gt/+}$ x *Rfx2*$^{gt/+}$ crosses

+/+	+/−	−/−
24 (27%)	43 (48%)	23 (26%)

Includes mice on both C57BL/6N and C57BL/6N x CD-1 backgrounds